

## Synthesis, Characterization, and Electrochemical Properties of Bis(2-benzimidazolylmethyl-6-sulfonate)amine-based zinc(II), copper(II), and oxidovanadium(IV) Complexes: SOD Scavenging, DNA binding, and Anticancer Activities

Mohamed M. Ibrahim<sup>1,2</sup>, Gaber A. M. Mersal<sup>1,3</sup>, Samir A. El-Shazly<sup>4,5</sup>, Abdel-Motaleb M. Ramadan<sup>2</sup>

<sup>1</sup> Department of Chemistry, Faculty of Science, Taif University, Taif, Saudi Arabia

<sup>2</sup> Department of Chemistry, Faculty of Science, Kafr El-Sheikh University, Egypt

<sup>3</sup> Department of Chemistry, Faculty of Science, South Valley University, Qena, Egypt

<sup>4</sup> Department of Biochemistry, Faculty of Veterinary Medicine, Kafr El-Sheikh University, Egypt

<sup>5</sup> Department of Biotechnology, Faculty of Science, Taif University, Taif, Saudi Arabia

\*E-mail: [ibrahim652001@yahoo.com](mailto:ibrahim652001@yahoo.com)

Received: 8 June 2012 / Accepted: 9 July 2012 / Published: 1 August 2012

---

The synthesis of a tridentate ligand, bis(2-benzimidazolylmethyl-6-sulfonate)amine H<sub>2</sub>SBz is described together with its zinc(II), copper(II), and oxidovanadium(IV) complexes [SBz-M(H<sub>2</sub>O)<sub>2</sub>] (M = Zn<sup>2+</sup> **1**, Cu<sup>2+</sup> **2**, and VO<sup>2+</sup> **3**). The ligand and its metal complexes **1-3** were characterized based on elemental analysis, conductivity measurements, spectral, and magnetic studies. The magnetic and spectroscopic data indicate a square pyramidal geometry is proposed for all complexes. The redox properties of the ligand and its complexes **1-3** were extensively investigated by using cyclic voltammetry. Complexes **1** and **2** exhibited quasi-reversible single electron transfer process. Whereas in complex **3**, only one electron oxidation peak was observed at + 0.72 V, which is due to the oxidation of V<sup>IV</sup> to V<sup>V</sup>. The SOD-like activity of complexes **2** and **3** has been investigated and showed that both complexes possess the capability to dismutase the superoxide anion generated in nitrobluetetrazolium/superoxide system. The electrochemical DNA binding studies by using oxidovanadium(IV) complex **3** was investigated and showed that the modified electrode with DNA causes the peak potentials,  $E_{pc}$ , and  $E_{pa}$  shifted to more positive values. This may be attributed to diffusion of the metal complex bound to the large, slowly diffusing DNA molecule and the resulted peak current due the equilibrium of free and DNA-bound oxidovanadium(IV) complex to the electrode surface. Complexes **2** and **3** were also assessed for their cancer chemotherapeutic potential towards colon cancer cell line (Caco-2) and showed that these complexes have the potential to act as an effective anticancer drug with IC<sub>50</sub> values of 4.0 and 2.5 μM for complexes **2** and **3**, respectively

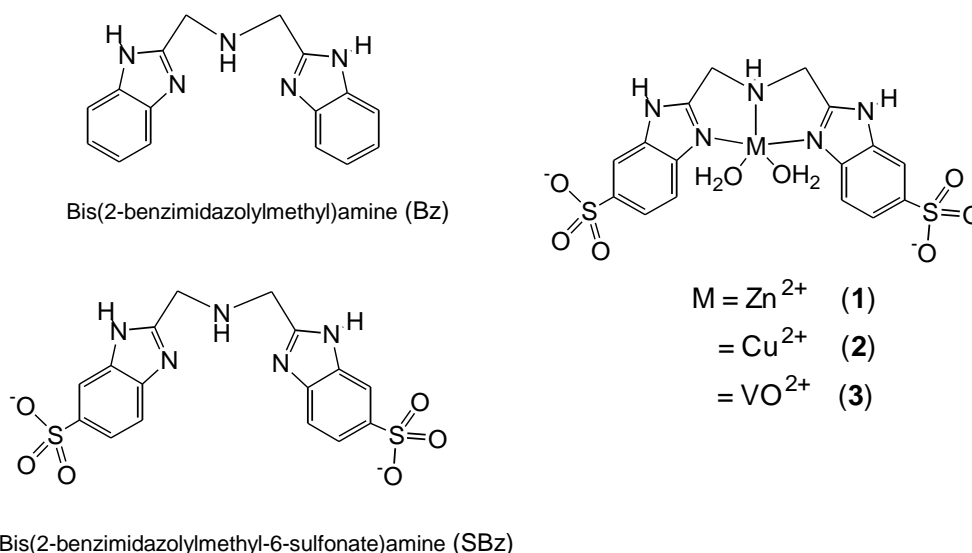
---

**Keywords:** Benzimidazole-containing ligand; Cyclic voltammetry; Electrochemical DNA binding studies; SOD mimic; Antitumor activities.

## 1. INTRODUCTION

The reactive superoxide free radical anion  $O_2^{\bullet-}$  is generated in cells as an avoidable sub-product of aerobic metabolism [1]. The intracellular concentration of  $O_2^{\bullet-}$  and consequently tissue damage is normally controlled by the superoxide dismutase (SODs), a group of metalloenzymes which play an important role in protecting cells through catalysis of superoxide disproportionation [2,3] into  $O_2$  and  $H_2O_2$  through a one-electron redox cycle involving its metal center. It is known that cancer cells have less than normal SODs activity and the treatment with bovine native Cu-SOD decreased the growth of several solid tumors [4].

It is difficult, however, to employ SODs because they are readily cleared by the kidney and are unable to enter cells because of their high molecular weight [5]. The presence of copper, manganese, and iron at the active site of SODs led many investigators [6-13] to search for low molecular weight complexes of these metals having SOD activity. Although many copper complexes catalyze the dismutation of  $O_2^{\bullet-}$  *in vitro* [14-21], their activities are attenuated *in vivo* by chelating agents ordinarily found in living cells [22]. Useful SOD mimics should be capable of crossing cell membranes and should be stable, active, and nontoxic. One general strategy for the research on new anticancer agents has been the therapeutic use of metal containing compounds [23,24]. Specially, in the search of less toxic metal-based antineoplastic drugs, essential metal complexes such as copper-based drugs have been developed [25]. The cytotoxicity of these complexes can be explained by different mechanisms of action. In particular, the report by Oberley and Buettner showed that cancer cells have a less than normal superoxide dismutase SODs activity and the treatment with bovine native Cu-SOD decreased the growth of several solid tumors [26].



Scheme 1. The ligand SBz and its metal complexes 1-3

The synthesis and study of structural models can lead the understanding of fundamental mechanistic aspects of enzymes as well as the development of structure reactivity relationship. The major task in designing these model compounds depends on the proper choice of ligands as well as the

steriochemical environment surrounding the metal centers. The water soluble ligand bis(2-benzimidazolylmethyl-6-sulfonate)amine, SBz is a tridentate NNN donor ligand (Scheme 1) with donor groups suitable placed for forming two five-membered chelate rings. The mononuclear complexes **1-3** show penta-coordinated metal ions with a square pyramidal coordination geometry. Herein we report the synthesis and structural characterization of new water soluble zinc(II), copper(II), and oxidovanadium(IV) complexes viz., [SBz-M(H<sub>2</sub>O)<sub>2</sub>] (M = Zn<sup>2+</sup> **1**, Cu<sup>2+</sup> **2**, and VO<sup>2+</sup> **3**). Since the possible biomimetic activity of metal complexes can be evaluated from the electrochemical behavior and spectroscopic studies. The electrochemical behavior of all complexes by cyclic voltammetry was studied because of their applications as SOD mimetic complexes are related to the redox properties, in which their general physicochemical and both SOD and cytotoxic activities were investigated.

## 2. EXPERIMENTAL

### 2.1. Materials and instrumentations

All chemical used were of analytical grad. The starting material, 4-sulfo-o-phenylenediamine was synthesized by the method of Nakata [27]. The IR spectra were recorded as KBr disks in the 4000-400 cm<sup>-1</sup> range on FT-IR Prestige-21 Shimadzu spectrophotometer. The electronic absorption spectra were obtained in methanolic solution with Shimadzu spectrophotometer UV-240. Magnetic moments were measured by Gouy's method at room temperature. ESR measurements of the polycrystalline samples at room temperature were made on Varian E9 X-band spectrometer using a quartz Dewar vessel. All spectra were calibrated with DPPH (g = 2.0027). The specific conductance of the complexes were measured using freshly prepared (0.001 M) solutions in the electrochemically pure MeOH or water at room temperature, using YSI Model 32 conductance meter. The copper content was determined by using atomic absorption technique, after destruction of the complexes with concentrated H<sub>2</sub>SO<sub>4</sub>/H<sub>2</sub>O<sub>2</sub> mixture.

### 2.2. Syntheses

#### 2.2.1. Synthesis of, N, N bis-(2-benzimidazolylmethyl-5(6)-sulfo)amine H<sub>2</sub>SBz

The ligand H<sub>2</sub>SBz was synthesized by the method of Nakata [27] as follows: 7.52 mmol (1.69 g) of 4-sulfo-o-phenylenediamine and 3.76 mmol (0.50 g) iminodiacetic acid in 150 mL 6 M HCl was stirred for 4 hours and cooled. The yielded blue precipitate was filtered, and dissolved in 0.1 M NaOH, decolorized on active carbon. After removing (filtering) the active carbon, 0.1 M HCl was added in little portions, and H<sub>2</sub>SBz precipitate was formed. 0.56 g (34% yield).

#### 2.2.2. Synthesis of the metal complexes **1-3**

A general procedure for the synthesis of the metal complexes **1-3** is as follows: a solution of 373 mg (1.0 mmol) of Zn(ClO<sub>4</sub>)<sub>2</sub> • 6H<sub>2</sub>O or 370 mg (1.0 mmol) of Cu(ClO<sub>4</sub>)<sub>2</sub> • 6H<sub>2</sub>O, or 163 mg (1.0

mmol) of  $\text{VO}_2\text{SO}_4$  dissolved in water (10 mL) was added to a solution of  $\text{Na}_2\text{SBz}$ , made up from (438 mg, 1.0 mmol) of the protonated ligand  $\text{H}_2\text{SBz}$  and  $\text{NaOH}$  (80 mg, 2.0 mmol) in water (10 mL). The resulting solution was stirred for 4 h at room temperature and then evaporated to dryness. yielded 0.427 mg (77%) of **1** as colorless crystals, 0.468 mg (82%) of **2** as blue crystals, and 0.426 mg (74%) of **3** as grey crystals.

### 2.3. Electrochemical measurements

The electrochemical behavior of the ligand SBz and its zinc(II), copper(II), and oxidovanadium(IV) complexes **1-3** was studied using cyclic voltammetry (CV) and square wave voltammetry (SWV) using auto lab potentiostat PGSTAT 302 (Eco Chemie, Utrecht, The Netherlands) driven by the General Purpose Electrochemical Systems data processing software (GPES, software version 4.9, Eco Chemie). The electrochemical cell used in this work contains three electrodes; platinum wire was used as a working electrode, SCE as a reference electrode, and a platinum wire was used as a counter electrode. Stock solutions of the ligand SBz and its complexes were freshly prepared daily in Britton–Robinson (BR). BR buffer was prepared via mixing 0.04 M  $\text{H}_3\text{BO}_3$ , 0.04 M  $\text{H}_3\text{PO}_4$ , and 0.04 M  $\text{CH}_3\text{COOH}$ . The desired pH was adjusted by the addition of 0.2 M  $\text{NaOH}$ .

### 2.4. SOD-like activity assay

The SOD-like activity of the two complexes were determined by NBT/NADH/PMS (Nitroblue Tetrazolium/reduced Nicotinamide/Phenazine methosulphate) system [28]. The superoxide radicals were produced by NADH, PMS and NBT in phosphate buffer (pH = 8.5). The concentration of the tested compounds varied from 1.0 to 10 mM. The amount of reduced NBT was spectrophotometrically at 560 nm by monitoring the increase in the concentration of blue formazan form for five minutes. The reduction rate of NBT was measured in the presence and absence of test compounds at various concentration of complex. All measurements were carried out at 25 °C using T80 spectrophotometer. The percentage inhibition (% of NBT reduction) was calculated using the following equation:

$$\% \text{ Inhibition of NBT reduction} = (\Delta A_{\text{control}} - \Delta A_{\text{Sample}} \times 100\%) / \Delta A_{\text{control}}$$

where  $\Delta A_{\text{control}}$  is the change in the absorbance at 560 nm over 5 minutes following the addition of PMS to the reaction mixture in the absence of complex sample. where  $\Delta A_{\text{Sample}}$  is the change in the absorbance at 560 nm over 5 minutes following the addition of PMS to the reaction mixture in the presence of complex sample. The SOD activity was expressed as a functional unite according to the following equation

$$\text{U/ml} = \% \text{ of inhibition} \times 3.75$$

### 2.5. Cell proliferation assay:

Cell proliferation studies were carried out using MTT assay. This assay is based on the capacity of mitochondrial lactate dehydrogenase enzymes (LDH) in living cells to convert the yellow water-soluble substrate 3-(4,5-dimethylthiazol-2-yl)-2,5-diphenyltetrazolium bromide to a dark blue

formazan product that is insoluble in water [30,31]. The proliferation inhibition ability of a representative of the prepared copper(II), and oxidovanadium(IV) complexes at different concentrations (0.3, 0.5, 0.6, 2.5, 5.0, and 10.0 mM) were verified using colon cancer cell line (Caco-2) obtained from VACSERA, Egypt. The MTT-developed color was measured at 570 nm using ELIZA microplate reader. The percentage of viable cells was calculated from the following formula: Survival fraction = OD of treatment cell/OD of control cells %. The IC<sub>50</sub> is the concentration of treatment required to induce 50% inhibition of cell growth, and the value was calculated by fitting the survival curve using graph pad prism software incorporated [31].

### 3. RESULTS AND DISCUSSION

#### 3.1. Characterization of the ligand H<sub>2</sub>SBz and its metal(II) complexes 1-3

The ligand bis(2-benzimidazolymethyl-6-sulfonate)amine, H<sub>2</sub>SBz is similar to the tridentate bis(2-benzimidazolymethyl)amine, Bz (Scheme 1), just sulfonate functions are formally introduced, was successfully synthesized by the method of Nakata et al. [27] from the reaction of iminodiacetic acid with two equimolar amounts of 4-sulfo-o-phenylenediamine in HCl (6N). Since the spectra resemble to that of Bz, other techniques such as elemental analysis and both FT-IR and Raman spectroscopies was also measured to confirm the presence of the sulfonate groups. Because of the electron withdrawing effect of the sulfonate groups, the chemical shifts of benzimidazole protons 4, 6 and 7 were shifted downfield by 0.46, 0.39 and 0.27 ppm, respectively. While in Bz, the protons 4, 7 and 5, 6 peaks were not separated, in SBz, the peaks of 4, 6, 7 protons were well separated. Differences are also well observed in <sup>13</sup>C NMR spectra, especially C5 (which is bound directly to the sulfonyl group) shifted downfield compared to Bz: the shift is 14.6 ppm. The obtained water soluble ligand SBz<sup>2-</sup> behaves as a tridentate ligand in the dianionic form.

**Table 1.** Molecular formulae, elemental analyses, and physical properties of the ligand SBz and its zinc(II), copper(II), and oxidovanadium complexes 1-3

Compound	Found (Calc.)%					$\Delta M(\Omega^{-1}cm^2mole^{-1})$
	%C	%H	%N	%S	%M	
H <sub>2</sub> SBz (C <sub>16</sub> H <sub>15</sub> N <sub>5</sub> O <sub>6</sub> S <sub>2</sub> )	43.76 (43.93)	3.39 (3.46)	15.89 (16.01)	14.43 (14.66)	-	-
[SBz-Zn(H <sub>2</sub> O) <sub>2</sub> ]•H <sub>2</sub> O (1) (C <sub>16</sub> H <sub>19</sub> N <sub>5</sub> O <sub>9</sub> S <sub>2</sub> Zn)	36.11 (36.64)	3.70 (3.45)	12.54 (12.62)	12.01 (11.56)	12.49 (11.78)	42
[SBz-Cu(H <sub>2</sub> O) <sub>2</sub> ]•2H <sub>2</sub> O (2) (C <sub>16</sub> H <sub>21</sub> N <sub>5</sub> O <sub>10</sub> S <sub>2</sub> Cu)	35.52 (35.65)	3.81 (3.71)	12.45 (12.26)	11.72 (11.23)	11.55 (11.13)	45
[SBz-VO(H <sub>2</sub> O) <sub>2</sub> ]•2H <sub>2</sub> O (3) (C <sub>16</sub> H <sub>21</sub> N <sub>5</sub> O <sub>11</sub> S <sub>2</sub> V)	35.01 (33.46)	3.68 (3.98)	12.19 (12.25)	11.16 (11.32)	8.87 (9.55)	39

**Table 2.**  $^1\text{H}$  NMR spectral data of the ligand SBz and its zinc(II) complex **1**.

Compound	$\delta(-\text{CH}_2)$		$\delta\{\text{SBz (H4/C4)}\}$		$\delta\{\text{SBz (H5/C5)}\}$		$\delta\{\text{SBz (H7/C7)}\}$		$\delta\{\text{SBz (C1/C2/C3)}\}$
	$^1\text{H}$	$^{13}\text{C}$	$^1\text{H}$	$^{13}\text{C}$	$^1\text{H}$	$^{13}\text{C}$	$^1\text{H}$	$^{13}\text{C}$	
SBz	4.00 (s, 4H)	54.01	7.51 (d, 2H)	116.14	7.62 (d, 2H)	118.33	7.97 (d, 2H)	124.28	136.25 147.11 150.12
<b>(1)</b>	4.21 (s, 4H)	58.21	7.59 (d, 2H)	117.83	7.78 (d, 2H)	120.41	8.03 (d, 2H)	125.32	137.94 148.24 152.83

$^1\text{H}/^{13}\text{C}$  NMR measurements were done in  $\text{D}_2\text{O}$  vs. DSS

Attempts have been made to synthesize zinc(II), copper(II), and oxidovanadium(IV) complexes of the ligand SBz. These complexes are then subjected to analytical studies for the elucidation of their structures. The reaction of perchlorate salts of  $\text{Zn}^{2+}$  and  $\text{Cu}^{2+}$ , as well as sulfate salt of  $\text{VO}^{2+}$  with the ligand in water in molar ratios of 1:1 at 30 °C led to the formation of three new complexes having different characteristics namely,  $[\text{SBzM}(\text{H}_2\text{O})_2]$  ( $\text{M} = \text{Zn}^{2+}$  **1**,  $\text{Cu}^{2+}$  **2**, and  $\text{VO}^{2+}$  **3**). They are soluble in  $\text{H}_2\text{O}$ , producing jelly solutions. The elemental analyses are in good agreement with the chemical formulae proposed for the compounds (Table 1).  $^1\text{H}$  NMR spectrum (Figure 1 and Table 2) of zinc(II) complexes **1** showed that the proton signals of both methylene and benzimidazole protons were shifted downfield in comparison to those of the ligand itself. Electrochemical measurements including cyclic voltammetry and electrical molar conductivity were studied. The conductivity values indicate the non-ionic nature of these complexes and they are considered as non-electrolyte. The electronic spectral and magnetic susceptibility measurements were used for assigning the stereochemistry of each complex. Electronic spectra indicate a square-pyramidal geometry for all complexes. This was also corroborated by the effective magnetic moment of the complexes.

### 3.1.1. FT-IR and Raman spectra of the ligand and its metal(II) complexes

The solid-state vibrational properties of the ligand  $\text{H}_2\text{SBz}$  and its zinc(II), copper(II), and oxovanadium(IV) complexes **1-3** were examined by FT-IR and Raman spectroscopies (Table 3). The IR spectrum of the ligand (Supplementary material, S1) exhibits two bands at  $3352\text{ cm}^{-1}$  and  $ca.1650\text{ cm}^{-1}$ , assigned to  $\nu(\text{NH})$  stretching and  $\delta(\text{NH})$  bending of the benzimidazole ring, respectively [32]. The spectrum of the free ligand also exhibits bands at  $3051$  and  $1560\text{ cm}^{-1}$  attributed to  $\nu(\text{N-H})$  and  $\nu(\text{C=N})$ , respectively. Two strong bands were also appeared in the IR spectrum of the ligand at  $1225$  and  $1175\text{ cm}^{-1}$ , assigned to asymmetric and symmetric stretching of  $\nu(\text{S=O})$ . Several strong bands also appeared in the range of  $1000\text{-}750\text{ cm}^{-1}$ , assigned to  $\nu(\text{S-O})$  stretching. The Raman spectrum of the ligand (Supplementary materials, S2) is just a characteristic of the strength of the vibration bond as IR absorption bands.

**Table 3.** The characteristic IR bands of the ligand SBz and its zinc(II), copper(II), and oxidovanadium complexes **1-3**.

Assignments	SBz	(1)	(2)	(3)
O-H (Coord. H <sub>2</sub> O)	-	3480	3510	3491
N-Hst (SBz)	3352	3357	3347	3349
N-Hst (2nd amine)	3051	3042	3046	3044
C-Hst (Aromatic)	2998	3001	2997	2998
C=Cst	1623	1625	1624	1623
N-Hdef	1531	1541	1547	1547
C-Hdef	1451	1463	1460	1455
S=Ost	1225&1175	1227&1175	1228&1174	1227&1178
C=Nst	1560	1566	1565	1568
=C-Hben	1096	1139	1147	1144
C-N=C (SBz)	1011	1034	1045	1039
S-Ost.	996	1010	1007	1008
V=Ost	967	973	969	971
M-N	-	457	446	463
M-O	-	526	553	581

The comparison of the IR spectrum of the ligand and its metal complexes indicated that the ligand acted as a tridentate ligand. The observed shifts in the stretching frequencies of  $\nu(\text{N-H})$  and  $\nu(\text{C=N})$  are indicative of the formation of these complexes. In given complexes **1-3**, the frequency of the  $\nu(\text{N-H})$  stretching vibration is lower in all complexes than in the free ligand. In analogous ammine complexes [33], the  $\nu(\text{N-H})$  stretching frequency becomes lower as the stability of the complex increases, indicating that the N-H bond is weaker in the complexes containing stronger M-N bonds. Increased strength of the metal-ligand bond means lower electron density on the nitrogen of NH group; this results in a decrease in the N-H bond strength, since nitrogen is the more electronegative atom in this bond. As a result of coordination, the stretching frequencies of the C=N bond in the imidazole unit of the benzimidazole rings shows opposite change. An upward shift (5-10  $\text{cm}^{-1}$ ) of  $\nu(\text{C=N})$  in the IR spectra of the complexes as compared to their values for the free ligand, suggesting coordination through the pyridine nitrogens of the benzimidazole rings [34]. The stretching bands of  $\nu(\text{S=O})$  and  $\nu(\text{S-O})$  showed slight shifts in all complexes. This may be due to their involvement in the hydrogen bonding with the water molecules. Owing to the heavy mass of the central atom and the relatively low order of the coordinated bonds, the corresponding stretching frequency appears in the low frequency region. So the conclusive evidence of the coordination of the dianionic SBz<sup>2-</sup> with the metal ions was shown by the appearance new bands at 435-583 and 410-581  $\text{cm}^{-1}$  assigned to the metal nitrogen (M—N) [35-37] and metal-oxygen (M—O) [33] vibrations, respectively. These bands were absent in the spectrum of the ligand itself, thus confirming participation of the O and N atoms in the coordination.

Oxidovanadium(IV) complexes can give rise either to monomeric structures with square pyramidal/trigonal bipyramidal/octahedral coordination geometry or to polymeric structures, involving  $\cdots\text{O}=\text{V}\cdots\text{V}=\text{O}\cdots$  linkages, with a distorted octahedral geometry [38]. However, on the basis of the location of the  $\nu(\text{V=O})$  band it is possible to distinguish between monomeric and polymeric complexes. In the present work, the oxidovanadium(IV) complex **3** exhibits a strong band in the region

959-988  $\text{cm}^{-1}$ , which has been assigned to  $\nu(\text{V}=\text{O})$  with a monomeric square pyramidal coordination geometry [39,40]. The bands observed in complex **3** in the region of 483-558  $\text{cm}^{-1}$  were also assigned to  $\nu(\text{V}-\text{N})$  while 455-458  $\text{cm}^{-1}$  are attributed to  $\nu(\text{V}-\text{O})$  [41].

In all complexes, a band of media intensity at 3480  $\text{cm}^{-1}$  with a shoulder at 3510  $\text{cm}^{-1}$  can be assigned to the asymmetric and symmetric  $\nu(\text{OH})$  stretching vibrations of the coordinated water molecules. The corresponding in-plane bending mode is probably overlapped to the very strong band at 1621  $\text{cm}^{-1}$ . One out-of-plane deformation mode of bonded water molecules could also be identified as a very weak signal at 786  $\text{cm}^{-1}$  [32]. The water coordinated as a true ligand in the inner sphere of the metal ion in all complexes can be recognized in the IR spectra by the appearance of the bands of the wagging, twisting, and rocking of the  $\text{M}-\text{OH}_2$  structural unit, established by the coordination of an oxygen electron pair to the metal ion. According to complexes **1-3**, a rocking vibration appears at 900  $\text{cm}^{-1}$ , a wagging vibration at 760  $\text{cm}^{-1}$ , and the metal-oxygen stretching vibration at 670  $\text{cm}^{-1}$ .

### 3.1.2. Zinc(II) titration of the ligand $\text{H}_2\text{SBz}$

The  $^1\text{H}$  NMR spectra of  $R (= [\text{Zn}^{2+}]_0 / [\text{SBz}]_0)$  dependence showed sharp peaks for  $R = 1.0$  is shown in Figure 1.

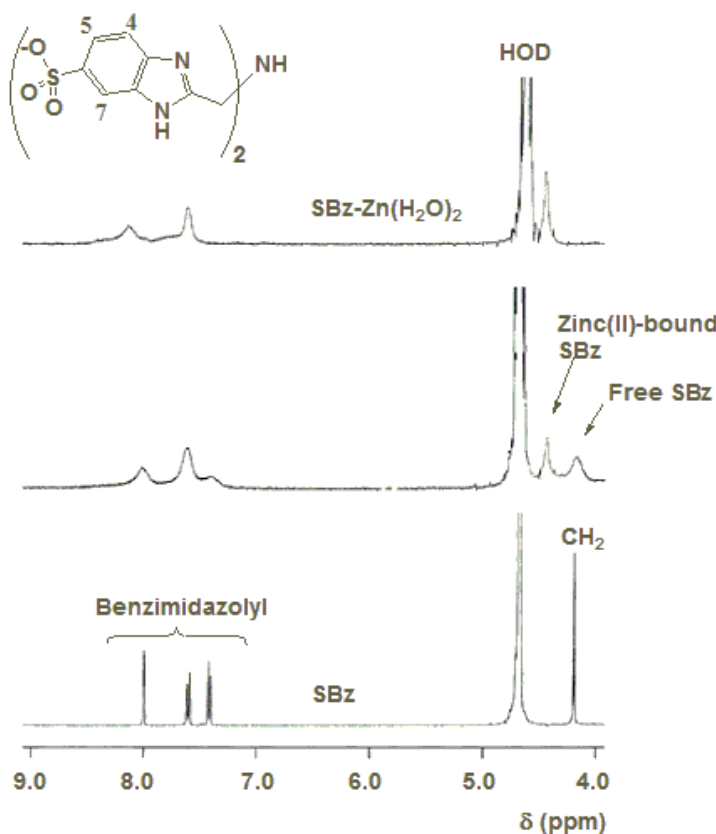


**Figure 1.**  $^1\text{H}$  NMR titration of the ligand SBz ( $2.0 \times 10^{-3}$  M) as a function of  $R (= [\text{Zn}^{2+}]_0 / [\text{SBz}]_0)$ :  $R = 0.0, 0.5,$  and  $1.0$  in  $\text{D}_2\text{O}$  at  $I = 0.1$  M  $\text{KNO}_3$  and  $25^\circ\text{C}$ .

Moreover, addition of excess of zinc(II) ions does not change the chemical shift, that is why formation of zinc complex with 1:1 stoichiometry is thought. This shows that in aqueous solution, the composition is [SBz-Zn(OH<sub>2</sub>)<sub>2</sub>], mononuclear model complex. Broadening of <sup>1</sup>H NMR peaks occurs between 0 < R < 1, because of the exchange reaction between the 1:1 complex and the free ligand. Broadening at R > 1 can be explained in terms of exchange reaction between the excess (and free) zinc ion and the 1:1 complex.

### 3.1.3. Electronic absorption spectra

The electronic absorption spectra of copper(II) **2** and oxovanadium(IV) **3** complexes were recorded in aqueous solution. The spectral data showed that, in the low energy region of the spectrum the oxidovanadium(IV) complex displays three low-intensity bands. The second of which is present as a shoulder in the 16949-18348 cm<sup>-1</sup> range. These bands can be assigned to <sup>2</sup>B<sub>2g</sub> → <sup>2</sup>E<sub>2g</sub>, <sup>2</sup>B<sub>2g</sub> → <sup>2</sup>B<sub>1g</sub> and <sup>2</sup>B<sub>2g</sub> → <sup>2</sup>A<sub>1g</sub> transitions respectively [42]. According to Ballhausen and others [43,44], these energy absorption bands are assigned to the ligand field transitions: d<sub>xy</sub> → (d<sub>xz</sub>, d<sub>yz</sub>), d<sub>xy</sub> → d<sub>x<sup>2</sup>-y<sup>2</sup></sub> and d<sub>xy</sub> → d<sub>z<sup>2</sup></sub> corresponding to b<sub>2</sub> → e\* (ν<sub>1</sub>), b<sub>2</sub> → b<sub>1</sub>\* (ν<sub>2</sub>) and b<sub>2</sub> → a<sub>1</sub>\* (ν<sub>3</sub>) transitions respectively in C<sub>4v</sub> symmetry [45]. These spectral characteristics suggest that the synthesized oxovanadium(IV) complex is five-coordinate, square-pyramidal structure [46-52].

Concerning copper(II) complex **2**, in square pyramidal copper(II) stereochemistry, the plausible d-orbital energy level scheme (idealized symmetry group C<sub>4v</sub>), is dx<sup>2</sup>-y<sup>2</sup> > dz<sup>2</sup> > d<sub>xy</sub> > d<sub>xz</sub>, d<sub>yz</sub>. Accordingly, the electronic spectrum of the five-coordinated copper(II) complex in the square-pyramidal geometry show three d-d bands [42]. These bands have been assigned to the transitions, dz<sup>2</sup> → dx<sup>2</sup>-y<sup>2</sup>, dxy → dx<sup>2</sup>-y<sup>2</sup>, and dxz, dyz → dx<sup>2</sup>-y<sup>2</sup>. The energy level sequence will depend on the amount of distortion due to ligand field and Jahn-Teller effect [42]. The electronic spectrum of the reported copper(II) complex shows two characteristic bands at 610 – 630 and 505 – 520 nm. These may be assigned to the dxz, dyz → dx<sup>2</sup>-y<sup>2</sup> and dxy → dx<sup>2</sup>-y<sup>2</sup>, transitions respectively. Because of the low intensity of dz<sup>2</sup> → dx<sup>2</sup>-y<sup>2</sup> transition, this band is usually not observed as a separate band in the tetragonally distorted complexes.

### 3.1.4. Magnetic studies

Oxidovanadium(IV) ion belongs to the 3d<sup>1</sup> and S=1/2 system [53]. The observed magnetic moments of the reported oxidovanadium(IV) complex at room temperature 2.15 BM (Table 4), corresponding to one unpaired electron and consistence with the mononuclear monomeric structure of this complex. This result is in accord with the fact that the spin-orbit coupling for oxidovanadium(IV) complexes is positive and the magnetically diluted oxidovanadium(IV) ion should exhibit magnetic moments very close to the spin-only value, as expected for a simple S=1/2 paramagnetic with d<sub>xy</sub> based ground state [54]. This normal magnetic moment excluded any significant interaction between neighboring oxidovanadium(IV) ions in the polycrystalline state [54]. This fact is also supported by the ESR spectral results, which give G-value equals 4.328, [G = (g<sub>||</sub> - 2)/(g<sub>⊥</sub> - 2)] > 4 [55]. According to

Hathaway *et al.* if the  $G > 4$ , the exchange interaction is negligible, while  $G < 4$  indicates considerable exchange interaction in the solid complexes [55].

**Table 4.** Magnetic moment values and ESR spectral data of complexes **2 & 3**

Complex		g <sub>1</sub>	g <sub>2</sub>	g <sub>3</sub>	R	μ <sub>eff</sub> (BM)
[SBz-Cu(H <sub>2</sub> O) <sub>2</sub> ] • 2H <sub>2</sub> O	(2)	2.336	2.196	2.092	0.6712	1.82
[SBz-VO(H <sub>2</sub> O) <sub>2</sub> ] • 2H <sub>2</sub> O	(3)	g <sub>  </sub> 2.277	g <sub>⊥</sub> 2.064	g <sub>av</sub> 2.135	G 4.328	2.15

For copper(II) complex, the room temperature magnetic moment is 1.82 BM corresponding to one unpaired electron [53,54] and consistency with the mononuclear monomeric structure of these complexes. This result is in accord with the fact that the spin-orbit coupling for copper(II) complexes is positive and the magnetically diluted copper(II) ion should exhibit magnetic moments very close to the spin-only value, as expected for a simple  $S=1/2$  paramagnetic with  $dx^2-y^2$  based ground state [53,54]. This normal magnetic moments excluded any significant interaction between neighboring copper(II) ions in the polycrystalline state [53,54]. This finding is further confirmed from the clear resolution of the ESR spectrum.

### 3.1.5. X-band ESR

The X-band ESR spectra of oxidovanadium(IV) and copper(II) complexes in the polycrystalline state have been recorded at room temperature. The ESR spectra are interpretable in terms of an effective spin of  $S = 1/2$ , and  $I = 7/2$ . The trend  $g_{||} (2.277) > g_{\perp} (2.064) > g_e (2.0023)$  (Table 4) observed for the investigated oxidovanadium(IV) complex shows that the unpaired electron of the  $d^1$  ( $VO^{2+}$ ) is located in the  $d_{xy}$  orbital and the spectral features are characteristic of axially elongated square pyramidal geometry [54]. These spectral features can be assigned unambiguously to oxidovanadium(IV) ions in the form of single and or pair ions by comparison with spectra of such species in other matrices [56,57]. As indicated by the magnetic moment measurements there seems to be no exchange interaction between the oxidovanadium(IV) ions in the solid state This fact is further confirmed by the ESR spectral data which give  $G$  values equals 4.328 [58]. This fact reveals that this complex is monomeric in nature and the metal - metal interactions are absent.

The spectral features of copper(II) complex exhibit intense ESR signals that are characteristic of the rhombic symmetry with the three  $g$ -values pattern. The three observed  $g$ -values ( $g_1$ ,  $g_2$ , and  $g_3$  in the order of decreasing magnitude) were computed from the spectrum. The two configurations square-pyramidal and trigonal bipyramidal are characterized by the ground state  $dx^2 - y^2$  and  $dz^2$  respectively [42]. EPR spectrum of copper(II) provides a very good basis for distinguish between these two general states. For the systems with  $g_3 (2.092) < g_2 (2.196) < g_1 (2.336)$ , the ratio of  $(g_2 - g_1)/(g_3 - g_2) = R$ , is a very useful for this purpose. If the ground state is  $dz^2$  the value of  $R$  is greater than 1. On the other hand, for the ground state being predominantly  $dx^2 - y^2$  the value of  $R$  is less than 1. Copper(II) complex shows the value of  $R$  (0.6712) less than 1, and this result confirms the five-coordinate square - pyramidal geometry.

### 3.1.6. Electrochemical studies of the Ligand SBz and its metal(II) complexes

In order to obtain additional experimental evidence that can explain the SOD-mimetic catalytic activity observed for the reported metal(II) complexes, we have also investigated their redox response by the cyclic voltammetry technique. Cyclic voltammograms were recorded in the aqueous solution vs Ag/AgCl reference electrode and scan rate of  $50 \text{ mVs}^{-1}$ . The employed potential range was (-1.2 – +1.2 V) in the presence of 0.1 M of tetrabutylammonium perchlorate (TBAP) as a supporting electrolyte. The obtained results of the ligand SBz are presented in Table 5. The cyclic voltammogram showed only one redox peak in the studied potential range (Figure 2) at  $\sim +0.54 \text{ V}$  for the oxidation peak and  $\sim +0.14 \text{ V}$  for the reduction peak. The peak separation potential  $\Delta E = (E_{\text{pa}} - E_{\text{pc}})$ , between the anodic and cathodic peaks is 400 mV. This large peak separation potential suggests that reaction is quasi-reversible behavior with a slow electron transfer.

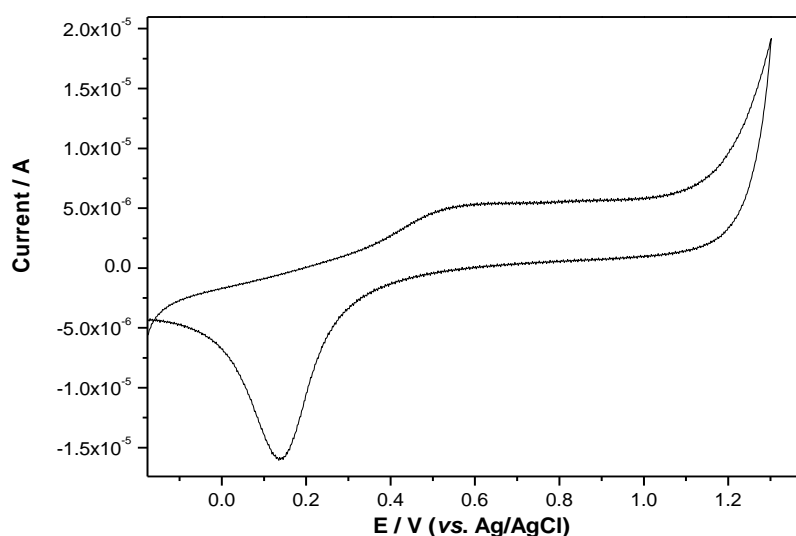


**Figure 2.** Cyclic voltammogram of the ligand SBz (1 mM) in BR buffer, pH=7.0 at Pt wire as a working electrode with scan rate of 50 mV/s.

**Table 5.** Voltammetric data for (2-benzimidazolylmethyl-6-sulfonate)amine in different scan rates

$\nu \text{ (V s}^{-1}\text{)}$	$E_{\text{pa}} / \text{V}$	$E_{\text{pc}} / \text{V}$	$\Delta E / \text{V}$	$E_{1/2} / \text{V}$	$i_{\text{pa}} / i_{\text{pc}}$
10	+ 0.43	+ 0.15	+ 0.28	+ 0.29	- 1.07
25	+ 0.49	+ 0.15	+ 0.34	+ 0.32	-0.34
50	+ 0.50	+ 0.14	+ 0.36	+ 0.32	-0.315
100	+ 0.54	+ 0.13	+ 0.41	+ 0.34	-0.299
150	+ 0.57	+ 0.12	+ 0.45	+ 0.345	-0.332
200	+ 0.59	+ 0.11	+ 0.48	+ 0.35	-0.349
250	+ 0.63	+ 0.11	+ 0.52	+ 0.37	-0.379
300	+ 0.66	+ 0.09	+ 0.57	+ 0.375	-0.377

The effect of scan rate on the oxidation and reduction peak potentials for the ligand SBz was also investigated (Table 5). The oxidation and reduction peak currents increased with the increase in scan rate values from 10 to 300 mV/s. The redox peak currents were proportional to the square root of the scan rate ( $v^{1/2}$ ) (Figure 3a-d), which, indicates that the electron transfer reaction is diffusion controlled. The linear regression equation was  $i_p$  (A) =  $9.72 \times 10^{-6} + 4.01 \times 10^{-6} V$  and  $i_p$  (A) =  $1.32 \times 10^{-6} + 7.3 \times 10^{-6} V$  with a 0.999 and 0.995 correlation coefficient for the oxidation and reduction peak currents, respectively. The effect of scan rate on the peak potential for the ligand was also investigated. By increasing the scan rate values, the anodic peak potentials shifted to more positive value and the cathodic peak potential shifted to more negative. The separation between the peak potentials,  $\Delta E$  by increasing the scan rate is a characteristic behavior for a quasi-reversible system.

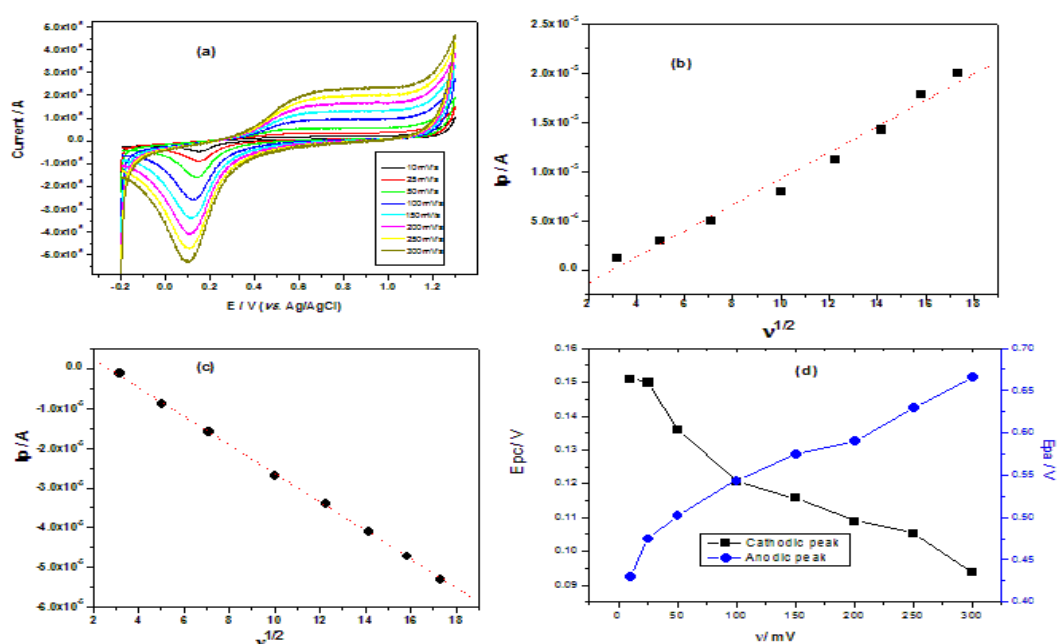


**Figure 3.** (a) Effect of scan rate on peak current height of the ligand SBz (b) Plot of anodic peak current ( $i_{pa}$ ) vs.  $v^{1/2}$ , (c) cathodic peak current ( $i_{pc}$ ) vs.  $v^{1/2}$  (d) The effect of scan rate on the peak positions.

Zinc(II) complex **1** (Figure 4a) exhibits a one-electron reduction peak at 0.0 and the corresponding oxidation occurs at 0.3 V (Table 6), which can be assigned to the formation of zinc(I) complex species. The investigated zinc(II) complex that undergoes reduction is completely regenerated following electrochemical oxidation. The value of the limiting peak-to-peak separation  $\Delta E_p$  (300 mV) slightly higher than the Nernstian value, for a reversible one-electron redox process. This finding suggests that the heterogeneous electron transfer process is easily reversible [59] ( $\Delta E_p$  60 mV for a reversible one-electron redox process) and not accompanied by stereochemical reorganization [60]. This suggests that  $Zn^{II}/Zn^I$  redox couple is quasi-reversible behavior with a slow electron transfer [61]. The same behavior was obtained for copper (II) complex (Figure 4b), where it also shows an additional

anodic peak in the forward scan and another cathodic peak in the reverse scan at + 0.14 V and + 0.13 V, respectively (Table 6). The redox peaks are attributed to the reduction of Cu(II) and Cu(I). The peak separation potential  $\Delta E_p = (E_{pa} - E_{pc})$  between the anodic and cathodic peaks is 270 mV. The large separation between the anodic and cathodic peaks in the redox couple suggests that Cu<sup>II</sup>/Cu<sup>I</sup> are also quasi-reversible behavior.

Axially coordinated secondary amine nitrogen atom has been suggested to have little influence on the redox properties of copper complexes [4]. Along these lines, if the coordinated nitrogen atom is replaced by solvent molecule, then the re reduction potential would be lower than the observed. The reason for the high potentials commonly found in the copper(II) with aliphatic amine donors has been attributed for some time due to the stabilization of the Cu(I) by the nitrogen donors relative to the stabilization of the Cu(II). The size of the chelate ring may also play an important factor which affects the electrochemistry of the copper complexes. Contiguous smaller chelate rings normally lower redox potentials for the Cu<sup>II</sup>/Cu<sup>I</sup> couple [62]. On comparing the  $E_{1/2}$  value for the copper(II) complex **2** with that for the [NSN-5,6] [Cu(-Biptb)](ClO<sub>4</sub>)<sub>2</sub>·2H<sub>2</sub>O, one observes that increasing the chelate ring size from five to six members has increased the potential by 60 mV.

The redox peaks of the ligand SBz were shifted to more negative value and a one electron oxidation peak was observed at + 0.72 V (Figure 4c). This may be due to metal-centered oxidation of V<sup>IV</sup> to V<sup>V</sup>, in which there appears not to be any change in the structure of parent complex when oxidized [63] and falls within the range reported in the literature for similar complexes [64]. The electrode process can therefore be represented as:  $[\text{VO}^{\text{IV}}\text{L}^2]^{\circ} \leftrightarrow [\text{VO}^{\text{V}}\text{L}^2]^+$ .

On the other hand, and taking into account the reduction potential of the couples O<sub>2</sub><sup>-</sup>/O<sub>2</sub><sup>2-</sup> and O<sub>2</sub>/O<sub>2</sub><sup>-</sup> (+0.98 and -0.45 V, PH = 7, respectively) [65], any redox pair with a intermediate potential value between these limits can act as a catalyst for the SOD reaction. The observed redox potential values ( $E_{1/2}$ ) of the reported complexes **2** and **3** lie in the middle of this range. Therefore, the electrochemical behavior observed for the investigated copper(II) and oxidovanadium(IV) complexes is in agreement with the results of the SOD like activity.

**Table 6.** Electrochemical data data for (2-benzimidazolylmethyl-6-sulfonate)amine and its zinc(II), copper (II) and oxidovanadium(IV) complexes (scan rate 100 V/s).

Compounds	SBz peaks					Complexes peaks				
	$E_{pa1}$ V	$E_{pc1}$ V	$\Delta E$ V	$E_{1/2}$ V	$i_{pa}/i_{pc}$	$E_{pa2}$ V	$E_{pc2}$ V	$\Delta E$ V	$E_{1/2}$ V	$i_{pa}/i_{pc}$
<b>SBz</b>	+ 0.54	+ 0.13	+ 0.41	+ 0.34	-0.299	-	-	-	-	-
(1)	+ 0.51	+ 0.11	+ 0.40	+ 0.31	0.2401	0.00	- 0.30	- 0.30	0.15	0.135
(2)	+ 0.46	+ 0.17	+ 0.39	+ 0.32	0.218	+ 0.13	- 0.13	+ 0.26	0.00	0.058
(3)	+ 0.14	- 0.22	+ 0.18	- 0.08	0.124	+ 0.72	-	-	-	-

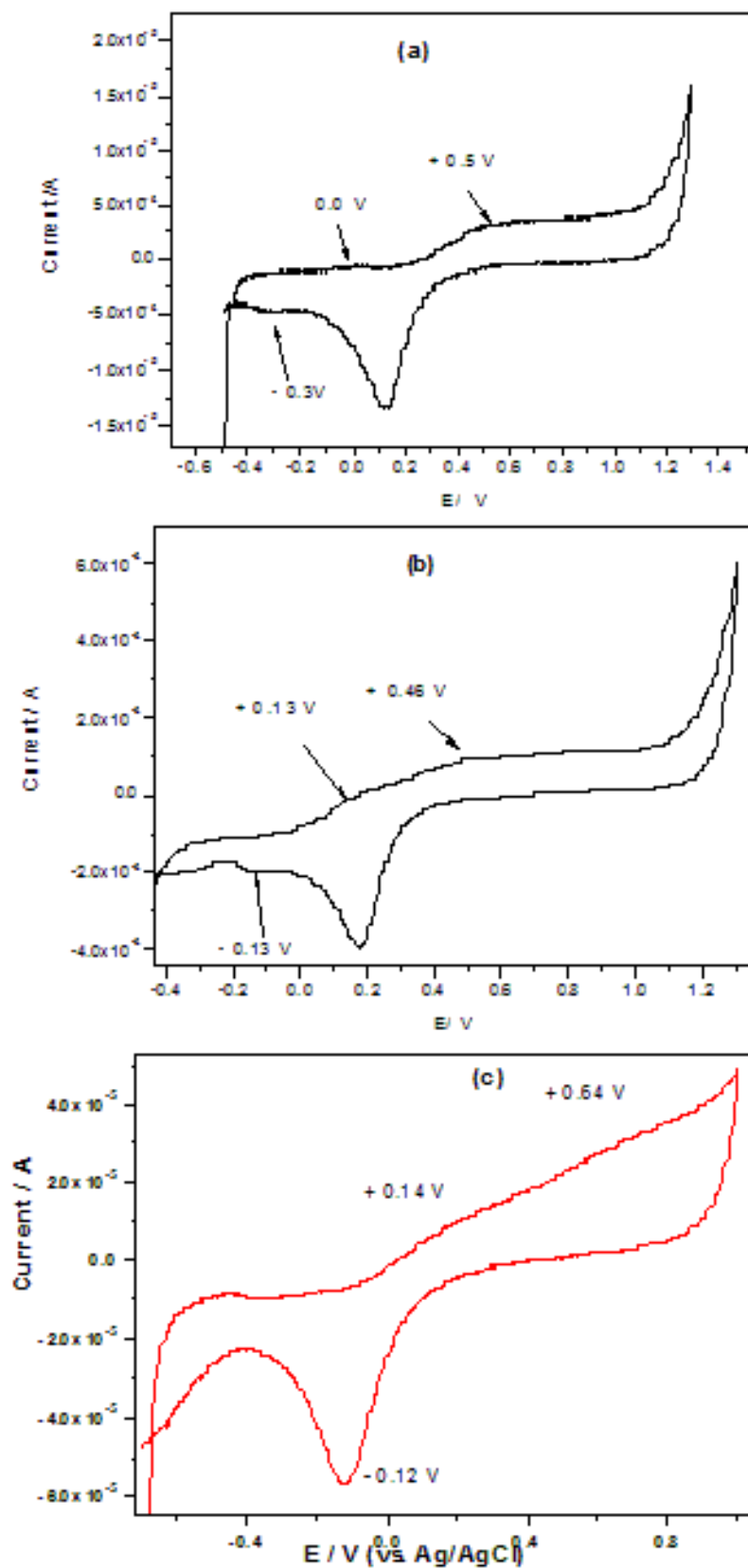


**Figure 4.** Cyclic voltammograms for (a) zinc(II) complex **1**, (b) copper(II) complex **2**, and (c) oxidovanadium(IV) complex in BR as a supporting electrolyte pH 7.0 using scan rate 50 mV/s.

### 3.2. SOD-mimetic activity

Superoxide anions have a very short half life and, accordingly, they must be produced continuously. In this colorimetric based assay, the kinetic investigations of  $O_2^-$  dismutation were conducted by varying the concentration of catalyst and phenathine methosulphate (PMS) as  $O_2^-$  photogenerator at 22 °C. Inhibition of the reduction of nitroblue tetrazolium (NBT) to formazan (F) by the reported copper(II) **2** and oxidovanadium(IV) **3** complexes was used for detection of the SOD-mimetic catalytic activity of these chelates in the phosphate buffer under similar biological conditions. As the reaction proceeding, the farmazan color is developed and the color changes from colorless to blue, which was associated with an increase in the absorbance at 560 nm. SOD reduces the superoxide ion concentration and thereby lowers the rate of formazan formation. In the SOD-like activity test, the metal complexes compete with NBT for oxidation of the generated superoxide ions. The more efficient the complex, the lower the concentration that corresponds to 50% inhibition of NBT reduction; this concentration is termed  $IC_{50}$  for comparative purposes. Figure 5 shows the percentage of inhibiting NBT reduction with an increase in the concentration of the metal complexes.

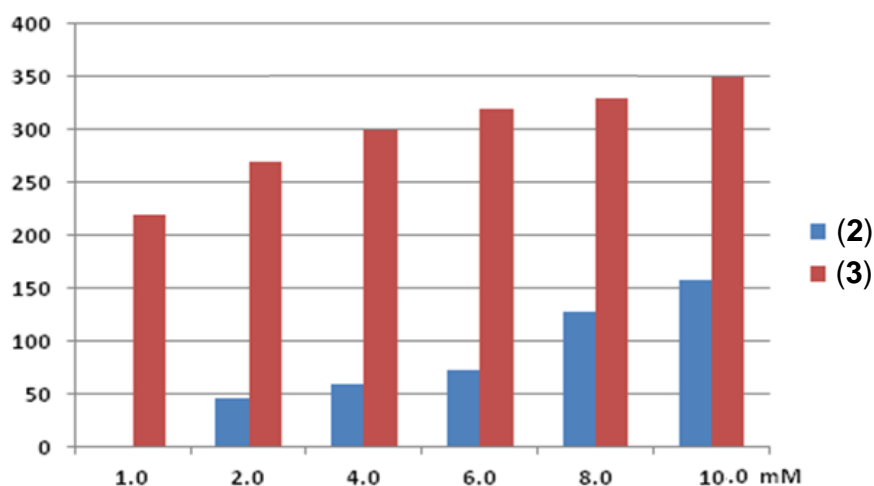


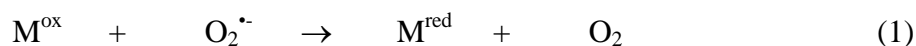
**Figure 5.** SOD activity expressed as U/ml using different concentrations of complexes **2** and **3**.

The data in Table 7 also reports the scavenging efficiency of each complex, giving its final concentration that produced efficient quenching of the superoxide anion radical. It also reveals that there are difference between the values of scavenging effectiveness and the catalytic constant of the complexes. This difference in the reactivates of these complexes can rationalized by means of correlation between the redox potential of the couples  $Cu^{II}/Cu^I$  and  $V^V/V^{IV}$  during the catalytic cycle and the SOD-mimetic activity. Although both complexes effects on the SOD activity becomes evident from the data presented in Table 7. Therefore, it seems necessary to investigate the behavior of a greater number of complexes of this type in order to attain a fuller understanding of this aspect.

**Table 7.** SOD-mimetic activity of complexes **2** and **3** at 25 °C.

Complex	[Cat] (mmol)	SOD (U/mL)
(2)	2.0	46.0
	4.0	59.0
	6.0	72.1
	8.0	127.0
	10.0	158.0
(3)	2.0	220
	4.0	270
	6.0	300
	8.0	320
	10.0	330

The good activities of the two complexes may be attributed to the flexible SBz ligand, which is able to accommodate the geometrical change from Cu<sup>II</sup> to Cu<sup>I</sup>, specially the two labile water molecules, which are proposed to be easily substituted by the substrate O<sub>2</sub><sup>•-</sup>, in the catalytic process, just like the O<sub>2</sub><sup>•-</sup>, in place of H<sub>2</sub>O bound to copper site in the mechanism of dismutation of O<sub>2</sub><sup>•-</sup> by native SOD. The mechanism proposed for the dismutation of superoxide anions by both superoxide dismutase and complexes **2** and **3** is thought to involve redox cycling of metal(I) ions (eqs. 1 and 2) [33]:



It has been proposed that electron transfer between copper(II) or oxidovanadium(IV) and superoxide anion radicals occurs through direct binding. The free axial site of the five-coordinate square pyramidal complexes is the likely attachment point for O<sub>2</sub><sup>•-</sup>, forming a six-coordinate adduct, which is highly unstable due Jahn-Teller effect [66]. As a consequence of this interaction, these ions undergo rapid reduction to copper(I) or oxidovanadium(V) with the release of O<sub>2</sub> molecule. It is assumed that electron transfer between the central metal and O<sub>2</sub><sup>•-</sup> occurs by direct binding [67]. The fast exchange of axial solvent molecules and a limited steric hindrance to the approach of the O<sub>2</sub><sup>•-</sup> in that complexes allow a better SOD mimic [68].

### 3.3. Electrochemical DNA binding studies

DNA-binding studies are important for the rational design and construction of new and more efficient drugs targeted to DNA [69]. A variety of small molecules interact reversibly with double-stranded DNA, primarily through binding interactions with two grooves of DNA double helix. So as to explore the mode of the oxidovanadium(II) complex binding to DNA, the electrochemical investigation of drug–DNA interactions can provide a useful complement to other methods and yield

information about the mechanism of interaction and the conformation of adduct [70]. Native DNA is not reducible at the electrode because the stability of the intact double helix makes the reducible bases inaccessible to the electrode. In DMF, the modified electrode with DNA causes all of the peak currents of complex **3** to decrease considerably. Additionally, the peak potentials,  $E_{pc}$ , and  $E_{pa}$ , both shifted to more positive values, shown in Figure 6. The decrease in peak currents can be attributed to diffusion of the metal complex bound to the large, slowly diffusing DNA molecule and the resulted peak current due the equilibrium of free and DNA-bound oxidovanadium(IV) complex to the electrode surface. We think that SBz-VO intercalates into the base pairs of DNA by the benzene planar [71]. Because of the intercalation, SBz-VO is not readily accessible to the electrode, thus causing the peak currents of the CV waves to diminish greatly. Moreover, the obvious positive shifts of peak potentials also indicate that this interaction mode may be intercalation between SBz-VO and DNA [72].

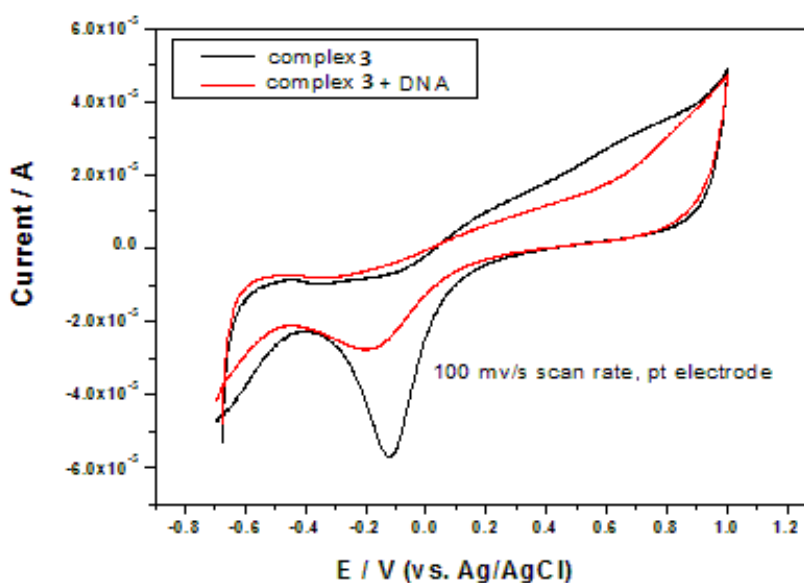


**Figure 6.** Cyclic voltammogram of oxidovanadium(IV) complex **3** (0.174 mM) (a) in the absence and (b) in the presence of DNA (0.30 mM nucleotide phosphate). Supporting electrolyte, 100 mM NaClO<sub>4</sub> in DMF, Sweep rate, 100 mV/s.

### 3.4. Cell proliferation studies

To further elucidate the anticancer ability of the reported copper (II) **2** and Oxidovanadium(IV) **3** complexes, the cytotoxicity assay was performed using Caco-2 colon cancer cell line. The potential effect of both complexes on the cell variability was evaluated by the reduction of tetrazolium salts MTT by mitochondrial dehydrogenase from metabolically active cells. The resulting optical density (OD) of soluble formazan product was measured spectrophotometrically at 570 nm (Figure 7). The results revealed that the *in vitro* study of the toxicity of both complexes indicate that they have potential to act as effective anticancer drug with IC<sub>50</sub> value of 4.0 and 2.5 mM for complexes **2** and **3**, respectively. Several mechanisms have been suggested to elucidate the anticancer activity of these

obtained complexes. Copper supplementation decrease the carcinogenic effect of many carcinogens possibly by promoting their metabolism. Treatment with tumor inducing 12-0-tetra-deconylphorbol-13-actate (TPA) depressed the total SOD activity in FFI fibroblast mouse epidermis, and human leukocyte. Also application of CuDIPS prior to TPA substantially reduced tumor incidence and yield. This anti-promoting property of CuDIPS could be attributed to its SOD-mimetic activity [73]. In accordance to the previous reported results and our result, which showed that the copper (II) complex has a SOD mimic activity it may also possible to hypothesis this mechanism [33]. Also these complexes may lead to increasing in the rate of radical formation leading to oxidative damage, resulting in disruption of lipid bilayers due to oxidation and cleavage of unsaturated fatty acid residues of phospholipids. Also they may act as a competitive inhibitors of de novo biosynthesis of purine nucleotides via the formation of a copper-substrate complex [74] or may result in internucleosomal DNA fragmentation [75]. Another possible mechanism is that the oxidovanadium(IV) compounds may also exert antiproliferative and cytotoxic effects via interactions with DNA. Vanadocene complexes interact with DNA's nucleotide phosphate groups forming a labile outer sphere complex via a water group.

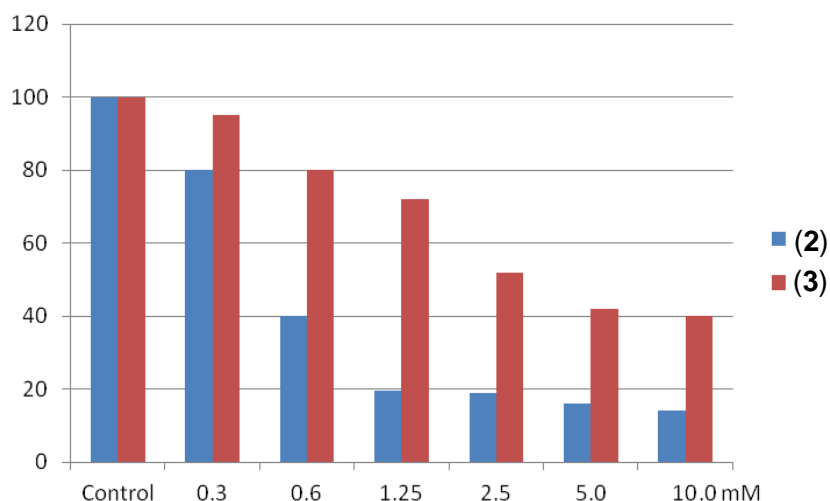


**Figure 7.** Colon cancer cell lines (Caco-2) were cultured (20,000 cells/well in 96-well tissue culture plates in a final 100  $\mu$ l/well) and incubated for 24 h at 37  $^{\circ}$ C and 5% CO<sub>2</sub> to obtain a monolayer, after which different concentrations of complexes **2** and **3** (10.0-0.312 mM) were added. After a 48-h incubation period (37  $^{\circ}$ C, 5% CO<sub>2</sub>), the cytotoxicity was assessed by MTT assays and cell viability were calculated relative to the untreated cells.

#### 4. CONCLUSION

Herein, we reported the synthesis of a new water soluble tridentate-containing ligand, namely bis(2-benzimidazolylmethyl-6-sulfonate)amine (H<sub>2</sub>SBz) together with its zinc(II), copper(II), and oxidovanadium(IV) complexes [SBz-M(H<sub>2</sub>O)<sub>2</sub>] (M = Zn<sup>2+</sup> **1**, Cu<sup>2+</sup> **2**, and VO<sup>2+</sup> **3**). Their structures and

properties were characterized by several physicochemical methods. A squar–pyramidal geometry is proposed for all complexes. The catalytic activity for the SOD reaction of the title compounds has been demonstrated by *in vitro* measurements. The observed redox processes of the metal centers lie in the middle of this range. Therefore, the electrochemical behaviors observed for these complexes are in agreement with this activity. The interactions between the oxidovanadium(IV) complex **3** and calf thymus DNA had been investigated using cyclic voltammetry. To further elucidate the anticancer ability of the reported complexes, the cytotoxicity assay was performed using Caco-2 colon cancer cell line. The obtained results indicate that both copper(II) and oxidovanadium(IV) complexes have good anti-cancer activity.

#### ACKNOWLEDGEMENT

This work was financially supported by Taif University, Saudi Arabia, Project No.: 1/1432/1274.

#### References

1. Fridovich, I. *Annu. Rev. Biochem.* 64 (1992) 97.
2. (a) D. P. Riley, *Chem. Rev.* 99 (1999) 2573; (b) D. Salvemini, D. P. Riley and S. Cuzzocrea, *Nat. Rev. Drug Discovery* 1 (2002) 367.
3. R. Krämer, *Angew. Chem., Int. Ed.* 39 (2000) 4469.
4. L.W. Oberly, G.R. Buettner, *Cancer Res.* 39 (1979) 1141.
5. W. Huber, M. G. P. Saifer, L. D. Williams, L. D. “*in Biological and Clinical Aspects of Superoxide and Superoxide Dismutase*” (Bannister, W. H., and Bannister, J. V., eds) Vol 11B, (1980) 395-407, Elsevier/North-Holland, New York.
6. J. Stein, J. P. Fackler, G. J. Jr. McClune, J. A. Fee, L. T. Chan, *Znorg. Chem.* 18 (1979) 3511.
7. S. W. C. Leuthauser, L. W. Oberley, T. D. Oberley, J. R. J. Sorenson, K. Ramakrishna, *J. Natl. Cancer Zmt.* 66 (1981) 1077.
8. F. A. Archibald, I. Fridovich, *J. Bacteriol.* 145 (1981) 442.
9. F. A. Archibald, I. Fridovich, *Arch. Biochem. Biophys.* 214 (1982) 452.
10. D. E. Cabelli, B. H. Bielski, *J. Phys. Chem.* 88 (1984) 3111.
11. D. E. Cabelli, B. H. Bielski, *J. Phys. Chem.* 88 (1984) 6291.
12. K. S. Yamaguchi, L. Spencer, D. T. Sawyer, *FEBS* 197 (1986) 248.
13. W. H. Koppenol, F. Levine, T. L. Hatmaker, J. Epp, J. D. Rush, *Arch. Biochem. Biophys.* 251 (1986) 594.
14. K. E. Joester, G. Jung, U. Weber, U. Weser, *FEBS Lett.* 25 (1972) 25.
15. D. K. Roth, J. Rabani, *J. Phys. Chem.* 80 (1976) 588.
16. M. Younes, U. Weser, *Biochem. Biophys. Res. Commun.* 78 (1977) 1247.
17. E. Lengfelder, C. Fuchs, M. Younes, U. Weser, *Biochim. Biophys. Acta* 567 (1997) 492.
18. S. Goldstein, G. Czapski, *J. Am. Chem. Soc.* 105 (1983) 7276.
19. E. Kimura, A. Yatsunami, A. Watanabe, R. Machida, T. Koike, H. Fujioka, Y. Kuramoto, M. Sumomogi, K. Kunimitsu, A. Yamashita, *Biochim. Biophys. Acta* 745 (1983) 37.
20. E. Kimura, T. Koike, Y. Shimizu, M. Kodama, *Inorg. Chem.* (1986) 2242.
21. W. M. Willingham, J. R. J. Sorenson, *Biochem. Biophys. Res. Commun.* 150 (1988) 252.
22. D. Darr, K. A. Zarilla, I. Fridovich, *Arch. Biochem. Biophys.* 258 (1987) 351.
23. G. Natile, M. Coluccia, *Coord. Chem. Rev.* 216–217 (2001) 383.
24. C. Orvig, M.J. Abrams, *Chem. Rev.* 99 (1999) 2201.
25. J. R. J. Sorenson, *Biology of Copper Complexes*, The Humana Press Inc., Clifton, (1987) 361.
26. L. W. Oberley, G. R. Buettner, *Cancer Res.* 39 (1979) 1141.

27. K. Nakata, M. K. Uddin, K. Ogawa, K. Ichikawa, *Chem. Lett.* (1997) 991.
28. M. Nishikim, N. A. Rao, K. Yogi, *Biochem Biophys Res. Commun.* 46 (1972) 849.
29. H. Aebi, *Method Enzymol* 105 (1984) 121.
30. T. Mosmann, *J. Immunol.* 65 (1983) 55
31. D. Gerlier, N. J. Thomasset, *Immunol. Methods* 94 (1986) 57
32. K. Nakamoto: *Infrared and Raman Spectra of Inorganic and Coordination Compounds*, Wiley, New York (1986) 324.
33. M. M. Ibrahim, A. M. Ramadan, G. A. M. mersal, S. Elshazly, *J. Mol. Struct.* 998 (2011) 1-10
34. V. K. H. Arali, V. K. Revankar, V. B. Mahale, P.J. Kulkarni, *Transition Met. Chem.* 19 (1994) 57.
35. D. G. Hill, A. F. Rosenberg, *J. Chem. Phys.* 22 (1954) 148.
36. D. G. Hill, A. F. Rosenberg, *J. Chem. Phys.* 24 (1956) 1219.
37. M. Kobayashi, J. Fujita, *J. Chem. Phys.* 23 (1955) 1354.
38. G. A. Kolawole, K.S. Patel, *J. Chem. Soc. (Dalton Trans.)* (1981) 1241.
39. J. Selbin, *Chem. Rev.* 65(2) (1965) 153.
40. R. C. Maurya, S. Rajput, *J. Mol. Str.* 794 (2006) 24.
41. P. E. Aranha, M. P. Do Santo, S. Romera, E.R. Dockal, *Polyhedron* 26 (2007) 1373.
42. A. B. P. Lever, *Inorganic Electronic Spectroscopy*, Elsevier, Amsterdam (1968).
43. C. J. Ballhausen and H. B. Gray, *Inorg. Chem.* 1 (1962) 111.
44. L. G. Vanquickenbourne and S. P. McGlynn, *Theor. Chim. Acta* 9 (1968) 390.
45. C. J. Ballhausen, *Introduction to Ligand Field Theory*, McGraw- Hill, New York, (1962).
46. M. Tumer, H. Koksall, M. K. Sener and S. Serin, *Transition Met. Chem.* 24 (1999) 414.
47. N. M. El-Metwally, Issam M. Gabr and A. A. El-Asmy, *Transition Met. Chem.* 31 (2006) 71.
48. S. Zhan and C. W. Yuan, *Transition Met. Chem.* 24 (1999) 277.
49. M. R. Maurya, Sweta Sikarwar and P. Manikandan, *Applide Catalysis A: General*, 315 (2006) 74.
50. N. Raman, S. J. Raja, J. Joseph, and J. D. Raja, *Russian journal of coordination chemistry.* 33 (2007) 7.
51. G. Asgedom, A. Sreedhara, J. Kivikoski, C. P. Rao, *Polyhedron* 16 (1997) 643.
52. K. S. Abu-Melha and N. M. El-Metwally, *Spectrochimica Acta Part A* 70 (2008) 277.
53. B. N. Figgis and J. Lewis, *Prog. Inorg. Chem.* 6 (1964) 37.
54. R. L. Dutta and A. Syamal, *Elements of Magnetochemistry*, Second Edt., Alffiliated East-West Press, Delhi (2007).
55. B. J. Hathaway, O. E. Billing, *Coord. Chem. Rev.* 5 (1970) 143.
56. B. T. Taker, A. Patel and L. Singh, *Transition Met. Chem.* 19 (1994) 623.
57. N. M. El-Metwally, I. M. Gabr, A. A. El-Asmy and A. A. Abou-Hussen, *Transition Met. Chem.* 31 (2006) 71
58. R. C. Aggarwal, N. K. Singh and R. P. Singh, *Inorg. Chem.* 20 (1981) 2794.
59. E. R. Brown, R. F. Large, in *Techniques of Chemistry: Physical Methods of Chemistry*, (Eds.: A. Weissberg, B. Rossiter); Wiely: New York (1971)
60. K. D. Karlin, P. L. Dahlstrom, J. R. Hyde and J. Zubieta, *J. Chem. Soc., Chem. Commun.* (1980) 906
61. (a) Z. Shirin, R. M. Mukherjee, *Polyhedron* 11 (1992) 2625; (b) A. Shyamala, A. R. Chakravarty, *Polyhedron* 12 (1993) 1545.
62. D. E. Nikles, M. J. Powers, F.L. Urbach, *Inorg. Chem.* 22 (1983) 3210
63. J. Dai, H. Wang, M. Mikuriya, *Polyhedron* 15 (1996) 1806.
64. A.H. Kianfar, S. Mohebbi, *J. Iran. Chem. Soc.* 4 (2007) 215
65. E. J. Ochiai, *Principles of Biochemistry of the Elements*, Plenum, New York (1987)
66. F. Cotton, G. Wilkinson, *Advanced Inorganic Chemistry*, Wiley, New York (1972).
67. J. A. Fee, *Metal Ions in Biological System*, H. Sigel, Ed., Marcel Dekker, New York (1981).
68. A. L. Abuhijteh, *J. Inorg. Biochem.* 68 (1997) 167.

69. M.J. Waring, in: G.C.K. Roberts (Ed.), *Drug Action at the Molecular Level*, Maemillar, London (1977) 167.
70. M.S. Ibrahim, *Anal. Chim. Acta* 443 (2001) 63.
71. M. T. Carter, A. J. Bard, *J. Am. Chem. Soc.* 109 (1987) 7528.
72. J. Sun, D.K.Y. Solaiman, *J. Inorg. Biochem.* 40 (1990) 271.
73. P. A. Egner, T. W. Kensler, *Carccarciinogenesis*. 6 (1985) 1167.
74. G. MacKenzie, A. Scott Frame, R. H. Wightman. *Tetrahedron* 27 (1996) 9219.
75. H. Zhou, Y. Lui, C. Zhen, Y. Gong, C. Wang, C. Zou, *Therm. Acta* 397 (2002) 87.